Solid State Communications 217 (2015) 38–42

Contents lists available at ScienceDirect

Solid State Communications

journal homepage: www.elsevier.com/locate/ssc

Design molecular rectifier and photodetector with all-boron fullerene

Zhi Yang [a,b,*], Yu-Long Ji [a], Guoqiang Lan [c], Li-Chun Xu [a], Xuguang Liu [d,e,**], Bingshe Xu [d]

[a] College of Physics and Optoelectronics, Taiyuan University of Technology, Taiyuan 030024, China
[b] Key Lab of Advanced Transducers and Intelligent Control System, Ministry of Education and Shanxi Province, Taiyuan University of Technology, Taiyuan 030024, China
[c] Department of Mining and Materials Engineering, McGill University, Montreal, Canada H3A 0C5
[d] Key Lab of Interface Science and Engineering in Advanced Materials, Ministry of Education, Taiyuan University of Technology, Taiyuan 030024, China
[e] College of Chemistry and Chemical Engineering, Taiyuan University of Technology, Taiyuan 030024, China

ARTICLE INFO

Article history:
Received 4 April 2015
Received in revised form
7 May 2015
Accepted 19 May 2015
Communicated by H. Akai
Available online 27 May 2015

Keywords:
A. Cluster
D. Transport properties
E. First-principles study

ABSTRACT

All-boron fullerene B_{40} is a highly stable molecule, which has been successfully synthesized in recent experiment. In this paper, with Au as two electrodes, the single-molecule device Au–B_{40}–Au was investigated by using density functional theory and non-equilibrium Green's function method. The results show that the device can exhibit large rectification ratio and significant negative differential resistance. More importantly, the photocurrent of the device has different responses in the infrared, visible and ultraviolet regions. The excellent optoelectronic properties ensure that the device can be used as photodetector.

1. Introduction

Fullerene molecules such as C_{60} and C_{70} have been the subject of intensive research during the past decades due to their intriguing structural, electronic and optical properties [1–10]. The search for possible fullerene-like molecules has attracted more and more attention. A promising candidate is the elemental boron cluster, since boron is the neighbor of carbon in the periodic table and has $2s^2 2p^1$ electronic configuration. For small boron clusters, however, the planar or quasi-planar structures have been proven to be stable because boron atom usually adopts sp^2 hybridization in the systems [11–15]. For example, Piazza and his coworkers suggested that, from both experimental and theoretical aspects, B_{36} is a highly stable quasi-planar cluster with a central hexagonal hole, and it can be viewed as a potential building block for constructing new two-dimensional materials [15].

Recently, all-boron fullerene, B_{40}, has been synthesized in experiment by Zhai and his co-workers [16]. B_{40} is a highly stable fullerene-like molecule with D_{2d} symmetry. Its structure is akin to a perforated red lantern, with two convex caps oriented perpendicularly and supported by four double-chain ribs. More interestingly, the energy gap between the highest occupied molecular orbital (HOMO) and the lowest unoccupied molecular orbital (LUMO) of B_{40} is 3.13 eV, well in the energy range of visible light (about 1.60–3.26 eV). The extraordinary structural and electronic properties of B_{40} make it a promising material for novel applications in, e.g., molecular electronics and optoelectronics.

In the paper, using density functional theory (DFT) and non-equilibrium Green's function (NEGF) method [17,18], we design single-molecule device with B_{40}, and investigate the transport and optoelectronic properties of the device. The material of this paper is organized as follows. Section 2 briefly describes the theoretical methods used in this work. In Section 3, we present our theoretical results. Finally, the conclusions of this work are summarized in Section 4.

2. Computational details

The structural optimization of B_{40} was performed by using DFT method as implemented in Atomistix ToolKit (ATK) package [19]. The exchange-correlation functional was treated within the generalized gradient approximation (GGA) proposed by Perdew, Burke and Ernzerhof (PBE) [20]. In addition, the double-ζ plus polarization (DZP) basis sets were employed in the calculation.

The electrical transport properties of the system were studied by using ATK, and the linear phase-coherent photocurrent I_{ph} was calculated with Nanodcal [21]. For the calculation of photocurrent,

* Corresponding author at: College of Physics and Optoelectronics, Taiyuan University of Technology, Taiyuan 030024, China
** Corresponding author.
E-mail addresses: yangzhi@tyut.edu.cn (Z. Yang), liuxuguang@tyut.edu.cn (X. Liu).

http://dx.doi.org/10.1016/j.ssc.2015.05.013
0038-1098/

the I_{ph} can be obtained from the following formula [22]:

$$I_{ph}=\frac{ie}{2\hbar}\int\frac{dE}{2\pi}Tr\{[\Gamma^{L}(E)-\Gamma^{R}(E)]G^{<}(E) +[f_{L}(E)\Gamma^{L}(E)-f_{R}(E)\Gamma^{R}(E)][G^{r}(E)-G^{a}(E)]\} \quad (1)$$

where $\Gamma^{L(R)}(E)$ is the self-energy function, representing the coupling between the central scattering region and the left (right) electrode; $G^{<}(E)$ is the lesser Green's function; $G^{r(a)}(E)$ is the retarded (advanced) Green's function; $f_{L(R)}(E)$ is the Fermi–Dirac distribution function of the left (right) electrode. It is easy to check that I_{ph} is proportional to the photon flux. Accordingly, we can define the photoresponse function f as

$$f=\frac{I_{ph}}{eF} \quad (2)$$

where F is the photon flux.

The optimized B_{40} and its HOMO and LUMO states are given Fig. 1a and b. We found that the calculated point group of free B_{40} is D_{2d}, and the symmetries of HOMO and LUMO are a_1 and b_2, respectively, in agreement with available data [16]. Because B_{40} has D_{2d} symmetry, with face-centered cubic (fcc) Au (001) surface as two electrodes, we designed two different configurations for single-molecule device Au–B_{40}–Au, i.e., the M1 and M2 in Fig. 1c. The M1 has mirror symmetry but the M2 is asymmetric. Compared with M1, in M2 the B_{40} molecule is rotated by 90° about the y axis.

It is well known that the choice of basis set is important for calculating the transport properties of the device. In recent studies [8,9], DZP basis set has been successfully employed to investigate the single-molecule devices with different-shaped Au electrodes. Therefore, we believe the basis set used in present study should be reasonable and reliable.

We also considered other possible configurations, but those configurations have higher energies and are therefore unfavorable. Furthermore, M2 is more stable than M1 by about 0.8 eV. In the rest of the paper, we mainly focus on the two most stable configurations.

3. Results and discussion

The calculated current–voltage (I–V_b) curves of the two configurations are shown in Fig. 2a. It is obvious that M1 and M2 have quite different I–V_b relationships. The mirror symmetry in M1 leads to an odd function, which means $I(V_b)=|I(-V_b)|$. In contrast, the I–V_b curve of M2 is more complicated. Firstly, the curve has totally different trends at negative and positive bias voltages. Secondly, when $V_b>0.8$ V, the current gradually decreases with V_b and a remarkable negative differential resistance (NDR) effect appears.

For a given V_b, the rectification ratio R can be defined as $R=I(V_b)/|I(-V_b)|$. The calculated R is shown in Fig. 2b. It is obvious that M1 cannot be used as molecular rectifier since $R\equiv 1$. For M2, however, the results show that it can be viewed as a typical molecular rectifier, and the largest rectification ratio is as high as 10.8 ($V_b=0.6$ V), which is larger than those of organic molecules such as $Mo_2Co(dpa)_4(NCS)_2$ ($R=4.8$, dpa=dipyridylamide) and polyyne-based molecular wires ($R=2.75$) [23,24]. Furthermore, the outstanding rectification ratio and NDR effect in M2 were also confirmed at local density approximation (LDA) level. Therefore, these properties are independent of the choice of calculation parameter, and are the intrinsic properties of the device. By changing the molecule–electrode contact, one can design molecular rectifier with B_{40} molecule.

To analyze the origination of the rectification ratio, the transmission spectra of M2 at $V_b=0, \pm 0.8$ V are shown in Fig. 2c. Because M2 is asymmetric, the transmission spectra are dependent on V_b, and they are quite different at V_b and $-V_b$. The narrow shapes of the transmission peaks indicate the interaction between Au surfaces and B_{40} should be weak. Similar phenomenon has also been observed in C_{60}-based device [7]. Under zero bias, only a few electrons transfer from Au electrons to B_{40}, owing to the electron deficiency of boron.

When $V_b=0$ V, there is no peak at Fermi level, indicating that the conductance is very low. It is worthy to note that at zero bias the transmission peak from the LUMO of B_{40} appears at about -0.6 eV, because there are additional electrons from Au surfaces reside on it (the transmission peak from the HOMO of B_{40} is not shown in Fig. 2c). When V_b increases to 0.8 V, the transmission peak of LUMO shifts into the bias window, which will open a transmission channel and significantly enhance the current. Accordingly, the main transmission channel of LUMO at $V_b=0.8$ V was found to be delocalized, as shown in Fig. 2d. The delocalized transmission channel ensures that the electron may pass through the device easily. Similar delocalized channel was also found for other positive bias voltages such as $V_b=0.6$ V (see Fig. 2d). As a result, the current under positive V_b is large. If V_b changes to -0.8 V, the transmission peak from the LUMO will move out of the bias window. In other words, there is no effective transmission channel as $V_b=-0.8$ V, finally leading to small current and large R.

Recently, Fan et al. investigated the current–voltage character of a single C_{60} molecule sandwiched between Au electrode and carbon nanotube electrode [10]. They found the system can exhibit rectification behavior. According to the above discussion, B_{40} molecule has become a powerful competitor to C_{60} molecule for designing new molecular devices.

Next we turn to discuss the optoelectronic properties of Au–B_{40}–Au device. Since the photocurrent I_{ph} is proportional to the photon flux F, we mainly focus on the photoresponse function f. The obtained f curves are shown in Fig. 3. It is worthy to note that, to produce a net dc electric current, a dipole potential is necessary for the photovoltaic process. For the single-molecule device studied here, it can be achieved by tuning local gate voltages. The schematic structure of the gate-controlled device is given in the inset of Fig. 3a. Two local gate electrodes, g1 and g2, are introduced in the device. The left and right electrodes extend to the electron reservoirs at $z=\pm\infty$ where photocurrent is collected. For the electromagnetic field of photon, only monochromatic plane wave was considered here for simplicity.

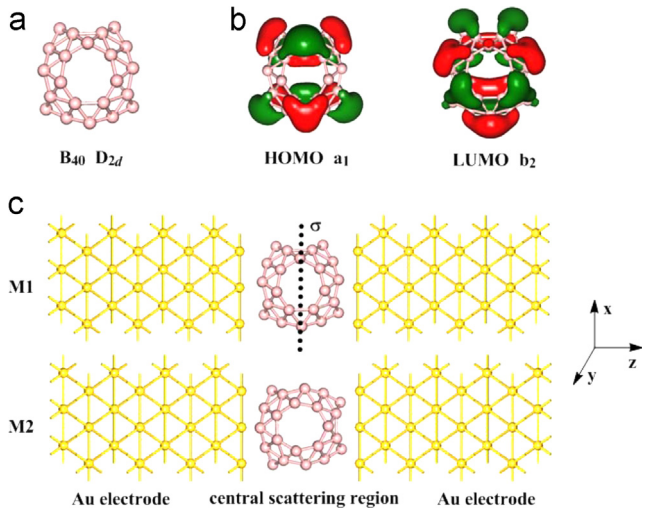

Fig. 1. (Color online) (a) The ground-state structure of B_{40}. (b) The HOMO and LUMO states of B_{40}. (c) Two different configurations of the single-molecule device Au–B_{40}–Au. The dashed line σ in M1 indicates mirror plane.